FULLY RUBBERY EPICARDIAL BIOELECTRONIC PATCH

Faheem Ershad[1], Kyoseung Sim[2], and Cunjiang Yu[1,3]
[1]Department of Biomedical Engineering, University of Houston, Houston, TX, 77204 USA
[2]Department of Chemistry, Ulsan National Institute of Science and Technology, KOREA and
[3]Department of Mechanical Engineering, University of Houston, Houston, TX, 77204 USA

ABSTRACT

The ideal epicardial bioelectronic patch should possess a cardiac tissue-like mechanical softness and deformability, and capability of spatiotemporal mapping of electrical and physical parameters. However, existing patches constructed from rigid materials with structurally engineered mechanical stretchability still form a hard–soft interface with the epicardium, which can strain cardiac tissue and does not allow for deformation with a beating heart. Alternatively, patches made from intrinsically soft materials lack spatiotemporal mapping or sensing capabilities. Here, we report the first epicardial bioelectronic patch that is made from materials that match the mechanical softness of heart tissue and is capable of multiplexed ECG mapping, strain and temperature sensing, electrical pacing, thermal ablation, and energy harvesting functions.

KEYWORDS

Epicardial bioelectronics, implantable, heart patch

INTRODUCTION

Implantable epicardial devices are important for discovering, monitoring, mitigating and treating cardiovascular diseases [1]. The devices can also provide therapeutic solutions [2]. The ideal bioelectronic device should possess cardiac-tissue-like mechanical softness and deformability, and various sensing functions. Specifically, the device should use soft materials with similar material properties to that of heart tissues in order to seamlessly interface with the epicardium and concurrently deform with a beating heart. It should also offer spatiotemporal mapping of the cardiac conduction characteristics and other physical parameters [3].

Advances in materials, mechanical structure designs, and bioelectronic technologies have led to the development of deformable epicardial bioelectronics. Structural engineering of rigid materials to yield mechanical softness has been an important strategy in the creation of soft epicardial devices [4]. These devices are difficult to interface with cardiomyocytes: flexible silicon electronics for cardiac mapping does not allow concurrent deformation with a beating heart [5] and mesh structured cardiac devices based on intrinsically rigid materials can overstrain cardiomyocytes [6]. Similarly, soft bioelectronics approaches typically use rigid, non-stretchy materials that form a hard–soft interface with biological tissues [7]. An alternative route is to use intrinsically soft materials. However, a cardiac wrap that is based solely on a continuous conductive material cannot provide spatiotemporal mapping capabilities [8].

In this Article, we report an epicardial bioelectronic patch that is made entirely of soft rubbery materials with moduli that are close to that of heart tissue (tens of kPa to ~1 MPa) [9]. The patch can monitor electrophysiological activity, strain and temperature, while deforming with a beating heart. The device contains a fully rubbery transistor array that is capable of mapping biopotentials in a spatial and temporal manner by using active-matrix multiplexing. The transistors are stable for a few weeks in biofluid due to encapsulation and the use of composite materials. The active matrix and a rubbery thermal actuator provide electrical pacing and thermal ablation capabilities, respectively, and a rubbery mechanoelectrical transducer allows for converting heart beats to electrical energy that could be potentially stored and utilized. An in vivo validation on a living porcine heart illustrates the key aspects and functionalities of the multifunctional rubbery epicardial bioelectronic patch.

RESULTS

Multifunctional rubbery epicardial bioelectronics

The epicardial bioelectronics was constructed into a thin elastic electronic sheet with sub-millimetre (~400 µm) thickness, based on rubbery conductors, semiconductors, and dielectrics developed through low-cost facile fabrication processes such as coating and printing. Figure 1a presents an exploded view of the soft, stretchy epicardial bioelectronic patch, which is fully made out of intrinsically soft and stretchable materials, including

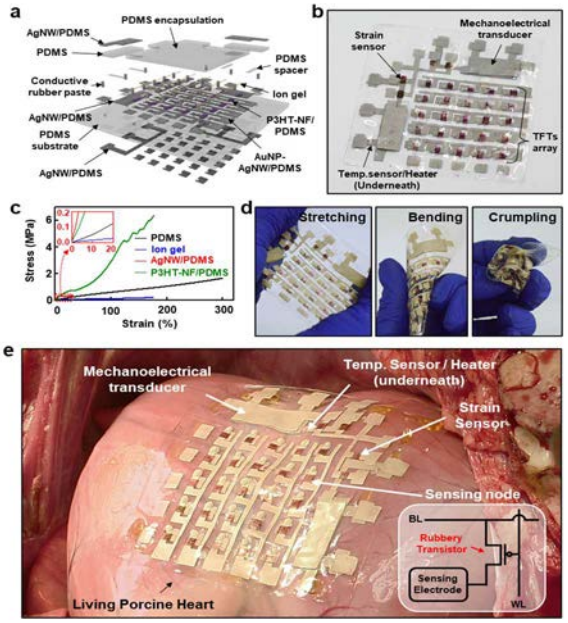

Figure 1: (a) Exploded schematic view of the rubbery epicardial patch. (b) Optical image of the epicardial patch. TFT, thin-film transistor. (c) Strain-stress curves of the rubbery components. (d) Rubbery epicardial patch under different mechanical deformations. (e) Rubbery epicardial patch on living porcine heart, inset shows circuit diagram for single node. BL, bit line; WL, word line.

polydimethylsiloxane (PDMS) as the substrate/encapsulation, conductive rubbery paste as interconnections, silver nanowires embedded in PDMS (AgNW/PDMS) as the rubbery conductor, poly(3-hexylthiophene-2,5-diyl) nanofibrils (P3HT-NF)/PDMS as the rubbery semiconductor, and ion gel as the rubbery dielectric. The fabricated epicardial bioelectronic patch is shown in Figure 1b. The bioelectronics was fabricated from double sided embedding of AgNW in thin PDMS (thickness of ~350 μm).

As emphasized earlier, the material stiffness should be like that of the native epicardium in order to allow for improved interfacing. The strain-stress curves of all materials used to construct the rubbery devices show excellent rubber-like mechanical softness with low Young's moduli of 6.60 MPa, 2.78 MPa, and 133 kPa, for the AgNW/PDMS conductor, P3HT-NF/PDMS semiconductor, and ion gel gate dielectric, respectively. All of the moduli are comparable to that of the commonly utilized elastomer PDMS as the substrate (15:1 weight ratio of base and curing agent, Young's modulus: 0.70 MPa) and porcine heart tissue, as shown in Figure 1c. Figure 1d shows various mechanical deformations of the epicardial bioelectronic patch, including stretching, bending, and crumpling. Owing to their mechanical softness, the devices can be conformally placed on the epicardial surface of a living porcine heart as demonstrated in Figure 1e. The rubbery active matrix multiplexed epicardial patch has 25 sensing nodes arranged in the format of a 5 × 5 array for mapping ECG. The individual sensing node is shown in the inset of Figure 1e.

Characterization of the rubbery devices

The rubbery transistor is the key component to construct an active-matrix array, enabling multiplexed spatial and temporal mapping of electrophysiological signals. Figure 2a shows the rubbery transistor and the output curves featuring typical p-channel characteristics. The rubbery transistor can be stretched by 30% and still function. It is noted that upon stretching, a slight change in field effect mobility (μ_{FE}), threshold voltage (V_{TH}), I_{on}/I_{off} from 1.245 $cm^2/V{\cdot}s$ to 0.579 $cm^2/V{\cdot}s$, -1.735 V to -1.678 V, and 5.247×10^3 to 9.243×10^2, respectively, and a moderate recovery of the values after releasing back to a strain of 0% are observed. The degradation is mainly due to the rupture of the P3HT-NF upon stretching [10].

Alongside monitoring the electrical activity of the heart, measuring the strain of the epicardium is another critical approach to examine cardiac health. Figure 2b shows the schematic exploded view (left) and optical image (right) of the rubbery strain sensor. The normalized resistance change depending on strain from 0% to 30% reveals high stretchability and a high gauge factor of 7.76 compared to the recently reported strain gauges used in cardiac health studies [4]. The response time of the strain sensor is 0.2 s.

Besides strain, temperature is another important cardiac parameter and can be used to unveil arrhythmias. The schematic illustration and optical image are shown in Figure 2c. Figure 2c also shows the normalized resistance change at different temperatures in the range of 27°C to 45°C under mechanical strains of 0% and 30%, which prove that there was no substantial impact on the sensing properties when deformed. The sensitivities of the rubbery temperature sensor were 0.35 %/°C and 0.38 %/°C under strains of 0% and 30%, respectively, which are comparable to metal thin film-based temperature sensors used for epicardial temperature monitoring [4]. The response time of the temperature sensor is 1.53 s.

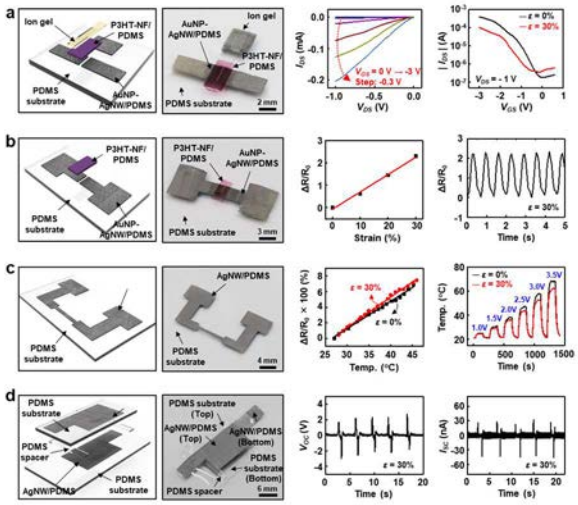

Figure 2: (a) Rubbery transistor schematic (left), optical image (middle), and IV characteristics (right). (b) Strain sensor schematic, optical image, and normalized resistance change characteristics. (c) Temperature sensor/thermal actuator schematic, optical image, and normalized resistance change/heating time characteristics. (d) Mechanoelectrical transducer schematic, optical image, and open-circuit voltage (V_{oc}) and short-circuit (I_{sc}) current characteristics.

Localized heating was also investigated as thermal ablation, which is a common treatment to destroy tissue that impedes the conduction system of the heart. The resistive thermal actuator was characterized by measuring the temperature change upon applying DC bias (ranging from 1 to 3.5 V) as shown in Figure 2 (rightmost). Typical Joule heating characteristics of around 68°C at 3.5 V can be produced, which is sufficient for thermal ablation.

Mechanoelectrical transducers that harvest heart beating could serve as possible and sustainable power sources for epicardial devices. All rubbery materials were used to construct the mechanoelectrical transducer, which operated based on the triboelectric effect in vertical contact-separation mode, shown in a schematic exploded view (left) and an optical image (right) in Figure 2d. Upon undergoing a mechanical strain of 30%, the open-circuit voltage (V_{oc}) and short-circuit current (I_{sc}) of the harvester reached ~1.47 V and ~86 nA, respectively, under a load resistance of 92 MΩ.

Rubbery active matrix for ECG sensor array

The rubbery transistor serves as a switching element in the active matrix for multiplexing. Figure 3a shows the representative images of the device in flat (top left), stretched (bottom left), and bent (right) states. The gain was maintained, and no significant voltage loss was observed under mechanical deformations including bending (R = 1.3 cm) and stretching (ε = 30%) as shown in Figure 3b.

Aside from the mechanical considerations, bio-fluids

are another factor that could potentially affect device performance. The rubbery transistor with a ~100 µm thick PDMS encapsulation layer was characterized by completely immersing the device into a phosphate buffered saline (PBS) solution maintained at a physiologically relevant temperature (37ºC). Figure 3c shows the optical image of the rubbery transistor in the PBS solution for the soaking test. As shown in Figure 3d, the device continued to operate normally with no substantial degradation of properties such as μ_{FE}, I_{on}, and I_{off}, for 46 days. Figure 3e shows the response of a sensing node based on the rubbery transistor in PBS after 46 days, which maintained a high gain of 0.866. All these results clearly prove the applicability and reliability of the rubbery transistor-based ECG sensing node for sustainable operation in the *in vivo* cardiac implantation.

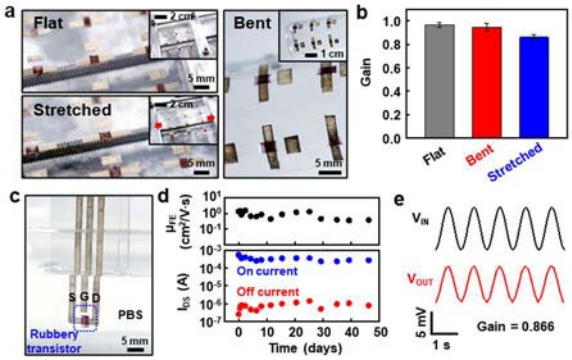

Figure 3: (a) Optical images of rubbery transistor under different mechanical deformations. (b) Input and output voltage ratio under mechanical deformations. (c) Rubbery transistor in phosphate buffered saline (PBS). (d) Mobility, drain current, and (e) gain after 46 days.

In vivo epicardial electrophysiological mapping

Spatial and temporal mapping over large areas of the heart can reveal portions of tissue that do not properly conduct the cardiac potential (e.g. scars). After locating the dysfunctional tissue, treatments such as local electrical pacing can be administered to restore normal cardiac functions. The 5 × 5 active matrix was implanted on an *in vivo* porcine heart for temporal potential mapping and electrical pacing. A surgical adhesive (BioGlue, CryoLife, Inc.) was applied between the device and porcine heart for enhanced adhesion. The electrophysiological signal mapping results from all 25 nodes are presented at five sequential time points of the sinus rhythm (Figure 4a). The sequential maps clearly show the anisotropic signal propagation from top to bottom, coinciding well with the spatial position of the rubbery active-matrix array on the porcine heart. Similar sequential maps at different time points during pacing are shown in Figure 4b. Based on the ECG traces from all 25 sensing nodes, isochronal activation maps were constructed to investigate the conduction velocities of the signal of the porcine heart for both the sinus rhythm (Figure 4c) and during pacing (Figure 4e). The relative activation delay depending on the distance for the sinus rhythm and during pacing are plotted in Figure 4d and 4f, respectively.

Based on the relative activation delay time, the obtained conduction velocity in the longitudinal direction (from top to bottom of the right ventricle) was 0.645 m/s and in the transverse direction (from left to right of the right ventricle) was 2.47 m/s. The results present the great potential of the mapping and pacing functions for advanced implantable biomedical devices that are not only limited to cardiac applications but can also be utilized for other organs that need to be spatially diagnosed and treated such as the brain, stomach, and bladder.

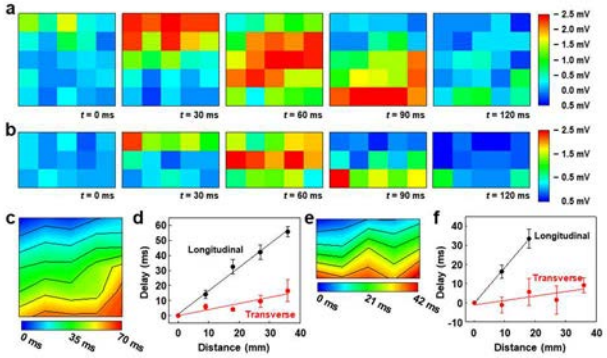

Figure 4: (a) In vivo electrophysiological mapping of the sinus rhythm at different sequential time points. (b) Mapping during pacing (two rows of the array were used to pace) at different sequential time points. (c) Isochronal activation plot during the sinus rhythm and (d) corresponding activation delay plot. (e) Isochronal activation plot during pacing and a(f) corresponding activation delay plot. The isochronal lines are drawn every 10 ms.

In vivo physical sensors and energy harvesters

Figure 5a shows the rubbery strain sensor implanted on the porcine heart *in vivo*. As shown in Figure 5b, the change in strain as the heart beats is clearly detected by the rubbery strain sensor, which reveals a normalized resistance variation of around 60%: this corresponds to a strain change of approximately 8% at systole according to the strain sensor calibration curve described above.

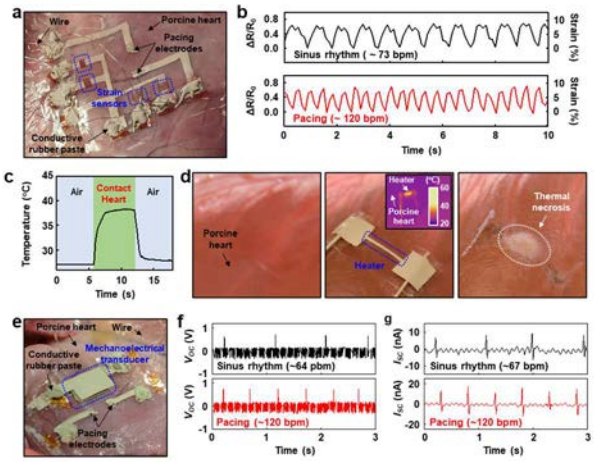

Figure 5: (a) Optical image of rubbery strain sensor on porcine heart. (b) Resistance change of rubbery strain sensor during sinus rhythm (top) and during pacing (bottom). (c) Temperature change upon contacting heart. (d) Thermal ablation on porcine heart. (e)Image of rubbery mechanoelectrical transducer on heart.(f) V_{oc} and (g) I_{sc} results during sinus rhythm (top) and pacing (bottom).

Epicardial temperature is also one of the crucial parameters for cardiac health monitoring. Figure 5c shows the temperature detected by the rubbery temperature sensor before and after contacting the porcine heart surface, demonstrating its excellent temperature sensing properties. By using the same structure, the temperature sensor can be used as a thermal actuator that is a useful tool for tissue necrosis and possibly tumour destruction. Figure 5d sequentially shows image of the epicardial surface before (left), during (middle), and after (right) thermal ablation by the rubbery thermal actuator: thermal necrosis can be clearly observed. The inset of Figure 5d (middle) shows the IR camera image of the thermal actuator generating around 60ºC, which is a sufficient temperature to cause necrosis (>50ºC).

As a proof-of-concept, *in vivo* implantation of the rubbery mechanoelectrical transducer onto a porcine heart was performed to evaluate its electrical output properties (Figure 5e). Figure 5f and 5g show the *in vivo* electrical output for the sinus rhythm and during pacing. The *in vivo* V_{oc} shows little change from 0.68 ± 0.03 V for the sinus rhythm to 0.74 ± 0.01 V during pacing, whereas the *in vivo* I_{sc} shows a relatively clear enhancement from 8.01 ± 1.17 nA for the sinus rhythm to 13.39 ± 2.59 nA during pacing. The energy scavenged from the mechanoelectrical transducer can be further optimized and managed to power the epicardial bioelectronic patch, potentially. These results corroborate the potential of the rubbery mechanoelectrical transducer as a power source to realize self-powered, implantable biomedical devices.

CONCLUSION

We have reported a soft and stretchable bioelectronic system consisting only of materials whose moduli are close to that of heart tissue. Unlike bioelectronics primarily based on rigid materials with mechanical structures that are stretchable on the macroscopic level, constructing bioelectronics out of materials with moduli matching those of the biological tissues suggests a promising route towards next-generational bioelectronics and biosensors that do not have a hard–soft interface for the heart and other organs. Our rubbery epicardial patch is capable of multiplexed ECG mapping, strain and temperature sensing, electrical pacing, thermal ablation, and energy harvesting functions, and we illustrated its capabilities on a living porcine heart. This combination of functions means that the device could potentially assist physicians in making decisions regarding the cardiac monitoring and treatment of patients and could potentially help accelerate the discovery of new remedies. While our bioelectronic patch is primarily intended as a temporary epicardial implant, the inclusion of anti-inflammatory agents and materials, and a careful investigation of induced fibrosis, could potentially lead to the development of a chronic implant.

ACKNOWLEDGEMENTS

C.Y. would like to thank the National Science Foundation CAREER grant (CMMI-1554499), Office of Naval Research grant (N00014-18-1-2338) under Young Investigator Program, National Institute Health grant (R21EB026175), and 3M non-tenured faculty award.

REFERENCES

[1] M. Heron, R. N. Anderson, and N. D. Brief, "Changes in the leading cause of death: recent patterns in heart disease and cancer mortality," *Cancer,* vol. 254, pp. 1-7, 2016.

[2] R. Dubois *et al.*, "Non-invasive cardiac mapping in clinical practice: Application to the ablation of cardiac arrhythmias," *Journal of Electrocardiology,* vol. 48, no. 6, pp. 966-974, 2015.

[3] F. Ershad, K. Sim, A. Thukral, Y. S. Zhang, and C. Yu, "Invited Article: Emerging soft bioelectronics for cardiac health diagnosis and treatment," *APL Materials,* vol. 7, no. 3, p. 031301, 2019/03/01 2018.

[4] D. H. Kim *et al.*, "Electronic sensor and actuator webs for large-area complex geometry cardiac mapping and therapy," *Proc Natl Acad Sci USA,* 10.1073/pnas.1205923109 vol. 109, no. 49, pp. 19910-5, Dec 4 2012.

[5] W. Lee *et al.*, "Nonthrombogenic, stretchable, active multielectrode array for electroanatomical mapping," *Science Advances,* vol. 4, no. 10, p. eaau2426, 2018.

[6] A. K. Blakney, M. D. Swartzlander, and S. J. Bryant, "The effects of substrate stiffness on the in vitro activation of macrophages and in vivo host response to poly(ethylene glycol)-based hydrogels," *Journal of Biomedical Materials Research Part A,* vol. 100A, no. 6, pp. 1375-1386, 2012/06/01 2012.

[7] J. Viventi *et al.*, "A conformal, bio-interfaced class of silicon electronics for mapping cardiac electrophysiology," *Science Translational Medicine,* 10.1126/scitranslmed.3000738 vol. 2, no. 24, p. 24ra22, Mar 24 2010.

[8] J. Park *et al.*, "Electromechanical cardioplasty using a wrapped elasto-conductive epicardial mesh," *Science Translational Medicine,* vol. 8, no. 344, p. 344ra86, 2016.

[9] L. Davenport Huyer *et al.*, "Highly Elastic and Moldable Polyester Biomaterial for Cardiac Tissue Engineering Applications," *ACS Biomaterials Science & Engineering,* vol. 2, no. 5, pp. 780-788, 2016/05/09 2016.

[10] H.-J. Kim, K. Sim, A. Thukral, and C. Yu, "Rubbery electronics and sensors from intrinsically stretchable elastomeric composites of semiconductors and conductors," *Science Advances,* 10.1126/sciadv.1701114 vol. 3, no. 9, p. e1701114, Sep 2017.

CONTACT

*C. YU, TEL: +1-713-1434487; YU.CUNJIANG@GMAIL.COM